



Corynebacterium glutamicum-mediated crystallization of silver ions through sorption and reduction processes

K. Sneha, M. Sathishkumar, J. Mao, I.S. Kwak, Y.-S. Yun*

Environmental Biotechnology National Research Laboratory, School of Chemical Engineering, Research Institute of Industrial Technology, Chonbuk National University, Jeonju 561-756, Republic of Korea

ARTICLE INFO

Article history:

Received 4 March 2010

Received in revised form 25 June 2010

Accepted 2 July 2010

Keywords:

Corynebacterium glutamicum

Active and inactive cells

Bioreduction

Biocrystallization

Silver nanoparticles

ABSTRACT

The processes of biosorption and bioreduction can provide important insights for understanding the mechanisms underlying the biosynthesis of nanoparticles. We performed various experiments using active/live and inactive/dead cells of *Corynebacterium glutamicum* to determine the capacity of these cells to adsorb and/or reduce silver ions. The biosorption of silver increased with increases in pH and equilibrium achieved within 30 min. The maximum experimental uptake with an initial silver concentration of 1000 mg/L was found to be 50.1 mg/g for active cells and 52.5 mg/g for inactive cells. After biosorption, we investigated the bioreduction capacity of both active and inactive cells of *C. glutamicum*. Strong plasmon resonance of silver nanoparticles was observed between 400 and 450 nm in the samples obtained from both active and inactive *C. glutamicum*. Transmission electron microscopy (TEM), energy dispersive X-ray (EDX) and X-ray diffraction (XRD) were performed to examine the formation of silver nanoparticles. A significant difference was noted in the formation of nanoparticles by live and inactive cells. A larger amount of reduction occurred on the surfaces of inactive cells. The nanoparticles formed were very irregular in shape and ranged in size from 5 to 50 nm. In the present study, the possibility of nanoparticles formation even in the absence of enzymes and metabolites has been studied. Crystallization of silver ions from aqueous solution by both active and inactive biomass can form a possible platform for a cost effective and eco friendly technique to remove or recover noble metals.

© 2010 Elsevier B.V. All rights reserved.

1. Introduction

Silver is used extensively as a raw material in various industries, because of its many advantageous properties such as malleability, ductility, photosensitivity, antimicrobial activity and electrical and thermal conductivity. Therefore, significant amounts of silver are discharged in the effluents from such industries [1]. The current processes used to recover silver can be economical when used on a large scale and if the metal concentration in the effluent is above 100 mg/L [2]. Significant amounts of silver in discharged industrial waste cause environmental toxicity and warrant removal from both the wastes and the environment. There is scope for further improvement in development of cost effective processes for harvesting noble metals from industrial waste. Existing physical and chemical technologies including chemical precipitation, electrocoagulation, membrane filtration and reverse osmosis are either too expensive or not suitable for treatment of dilute solutions [3].

Adsorption technologies using activated carbon appear to be very promising for silver recovery. However, the high cost of

preparing the necessary carbon is a major limiting factor [4]. Efforts are being made to recover silver from industrial effluents by means of bioremediation, since microbes contain metal-binding sites that can be used in environmental decontamination [5]. Studies of Ag⁺ biosorption using *Thiobacillus* sp. and *Cladosporium* sp. were conducted by Pethkar et al. [6], and similar studies were performed by Gomes et al. [7] using various strains of *Rhodotorula mucilaginosa* as a biosorbent. Though biosorption has been used in bioremediation applications, few studies have analyzed the byproducts of biosorption of metals by microorganisms. In addition, microbes are potent eco-friendly nanomaterial synthesis factories [8]. Nanotechnology is emerging as a cutting-edge technology, which will play a crucial role in this millennium. Unlike bulk materials, nanoparticles exhibit characteristic physical, chemical, optical, magnetic, and thermal properties [8,9]. In context of the current drive to synthesize green chemistry methods for nanomaterials fabrication, biological systems are of significant interest [8]. The biological systems of the microbes provide an ambient chemical system for synthesizing a wide range of inorganic nanomaterials. In particular, many bacterial species are known to reduce the ionic forms of noble metals to the zero valent forms in nanosize [10]. The nanoparticle synthesis occurs intracellularly or extracellularly in organisms [11,12]. Though many general reports about the mechanism of

* Corresponding author. Tel.: +82 63 270 2308; fax: +82 63 270 2306.
E-mail address: ysyun@chonbuk.ac.kr (Y.-S. Yun).

metal nanoparticle formation are available, the exact mechanism leading to their formation is not yet completely understood. It has been proven that metals are initially bioadsorbed/bioaccumulated and then reduced to a zero valent form by the microbes as part of a defense mechanism. Numerous studies have confirmed that bioreduction can be caused by two mechanisms: enzymatic catalysis and non-enzymatic reduction [13]. Lin et al. [14] studied non-enzymatic reduction and the results indicated that certain organic functional groups on microbial cell walls could be responsible for the reduction process under certain conditions. Mouxing et al. [15] developed a process for Ag nanoparticle synthesis by bioreduction of $[\text{Ag}(\text{NH}_3)_2]^+$ to Ag^0 using *Aeromonas* sp. Fu et al. [16,17] demonstrated that dried cells of *Bacillus megaterium* DOI and *Lactobacillus* sp. A09 are capable of reducing silver ions through the interaction between silver ions and the functional groups on the microbial cell wall. *Verticillium* sp. and *Fusarium oxysporum* are also novel organisms for the extracellular synthesis of nanoparticles and have the potential for easy downstream processing [18]. A recent report by Binupriya et al. demonstrated that both live and dead biomass filtrates of *Aspergillus oryzae* var. *viridis* could synthesize gold and silver nanoparticles. They also explained the involvement of organics from dead cells, in crystallization of silver nanoparticles [19,20]. Zhang et al. [13] studied the biosorption and bioreduction of diamine silver complex using live *Corynebacterium* sp. leading to the formation of silver nanocrystals that were 10–15 nm in diameter. They also proved the absence of bioreduction of silver ions of silver nitrate. The studies noted above clearly indicate that the biosorption and bioreduction of metals are linked, but most of the reports do not completely explain the link between the two processes. In addition, there are not many reports available on biosorption-coupled bioreduction processes in active and inactive cells. Therefore, the investigation of biosorption-coupled bioreduction can provide insight into the mechanisms of the enzymatic and non-enzymatic processes involved in the biosynthesis of nanoparticles.

C. glutamicum, a gram-positive bacterium, is being used in a lysine fermentation industry and its waste biomass is generated in a large amount. The waste biomass has been used in studies of dye and metal absorption. Potentiometric titration and Fourier transform infrared spectroscopy (FT-IR) studies have revealed that the cell wall of *C. glutamicum* is comprised mainly of carboxyl, phosphonate and amide groups [21], where negatively charged groups can easily absorb positively charged Ag^+ ions. The main aim of this study is to scrutinize the percentage conversion of biosorbed ions to bioreduced ions. Herein, we for the first time have compared the biosorption-coupled bioreduction capacity of both active and inactive biomasses.

2. Materials and methods

2.1. Bacterial strain and culture conditions

C. glutamicum (ATCC 13032), obtained from Korean culture center of microorganisms, was stored at 4 °C and subcultured once per month on Luria–Bertani (LB) agar plates. A starter culture was developed by transferring one full loop of the organism from the nutrient agar to 100 mL of LB broth in an Erlenmeyer flask and incubated at 30 °C under shaking at 160 rpm. After 24 h, 10 mL of the starter culture was transferred to an Erlenmeyer flask containing 1 L of LB broth for inoculum development and it was incubated for 24 h at 30 °C in an orbital shaker at 170 rpm.

2.2. Preparation of the biosorbent

The active biomass of *C. glutamicum* was centrifuged at 8000 rpm for 15 min in a refrigerated centrifuge after 24 h of incu-

bation. The biomass was washed twice with sterile double distilled water to separate it from the other media components. Active biomass was obtained by pelleting the washed biomass. Inactive biomass was prepared by resuspending the pellets of active cells in sterile double distilled water, followed by autoclaving at 121 °C for 15 min, at 15 psi. Then the heat killed cells were centrifuged at 8000 rpm for 15 min, for obtaining inactive biomass. Freshly prepared biomass was used for each set of experiments.

2.3. Determination of biosorption capacity

2.3.1. Effect of pH on biosorption by active and inactive biomass

Batch experiments were conducted in a series of Erlenmeyer flasks containing 20 mL of 1000 mg/L silver nitrate solution and 0.2 g of wet biomass with an adjusted pH in the range of 1–7 in order to determine the optimum pH level for silver biosorption by active and inactive *C. glutamicum*. The silver nitrate–biosorbent mixture was placed on a rotary shaker at 30 °C and 160 rpm in dark conditions. The pH of the silver ion–biomass suspension was continuously monitored for 6 h and a constant pH level was maintained by the addition of 1 N HNO_3 or NaOH. After 6 h, the samples were centrifuged at 12,000 rpm for 10 min and the supernatant was collected. The remnant Ag^+ concentration in the supernatant was analyzed by inductively coupled plasma spectroscopy (ICP) (Agilent 7500).

2.3.2. Biosorption isotherm of active and inactive biomass

Sorption experiments were carried out using 0.2 g of active and inactive cells in combination with 20 mL AgNO_3 solution with concentrations of Ag^+ varying from 100 to 1000 mg/L in order to study the adsorption capacity of the biosorbents. The reaction was allowed to take place 6 h with shaking at 160 rpm at a natural pH (6.04 ± 0.2) level and 30 °C. The supernatant was separated from the cells by centrifugation at 12,000 rpm for 10 min. ICP analysis was then performed to determine the ion concentration of the remnant Ag^+ . After ICP analysis, Langmuir and Freundlich equations were used to describe the equilibrium biosorption.

2.3.3. Effect of contact time on biosorption

In order to determine the kinetics of the Ag^+ uptake from the solution, experiments were conducted at an initial concentration of 1000 mg/L for both active and inactive cells. Samples were collected at predetermined intervals and the bacterial cells were promptly separated from the salt solution by centrifugation at 12,000 rpm for 10 min. The supernatant was collected for ICP analysis to determine the residual Ag^+ concentration.

2.3.4. Data evaluations

The amount of metal adsorbed (Q , mg/g) by active and inactive bacterial biomass was calculated using the following equation:

$$Q = \frac{(C_i - C_f)V}{m} \quad (1)$$

where C_i and C_f are the initial and the equilibrium concentrations (mg/L), respectively, V is the working volume of the solution (L) and m is the weight of the biomass (g).

2.4. Determination of bioreduction

Experiments were carried out by suspending 10 g/L of wet, active and inactive biomass in aqueous silver nitrate solutions containing 1000 mg/L of silver. These suspensions were kept in the dark under shaking conditions. Samples were taken at regular intervals and examined using a spectrophotometer to detect the formation of Ag nanoparticles. After bioreduction, the suspension was centrifuged and the sample was subjected to TEM analysis, energy

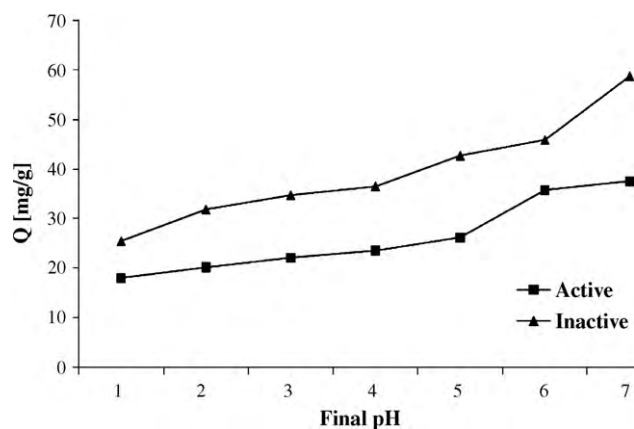


Fig. 1. Effect of pH on silver adsorption by active and inactive *Corynebacterium glutamicum* biomasses.

dispersive X-ray (EDX) and X-ray diffractograms (D/Max 2005, Rigaku) in order to detect the formation of silver nanoparticles. The residual silver concentration was analyzed using ICP analysis. TEM images of silver nanoparticles synthesized by active and inactive cells were observed without separation of the nanoparticles from the cell and the culture supernatant. TEM samples of the aqueous suspension containing Ag nanoparticles were prepared by placing a drop of the suspension on carbon-coated copper grids. The films on the TEM grids were allowed to stand for 2 min, after which the extra solution was removed using blotting paper and the grid was allowed to dry prior to measurement. TEM observations were performed on a HITACHI-JP/H7600 instrument (Japan) operated at an accelerating voltage of 100 kV. EDX analyses were performed on a JEOL JSM-6400 microscope (Japan) fitted with an Oxford-6506 (England) EDX analyzer.

3. Results and discussion

3.1. Effect of pH

The pH of the solution normally has a major role to play in the biosorption of metal species [21]. An increase in pH increased the biosorption of silver ions (Fig. 1). The prime reason for poor uptake of silver ions at acidic pH levels was the competition between the protons and silver ions to occupy the binding sites. Even though an increase in adsorption with an increase in pH was observed, experiments with a pH value higher than 7 were not completed. This was due to the fact that silver tends to precipitate in alkaline pH, which could be due to the formation of silver hydroxides. Lin et al. [22] described that at pH higher than 4, the carboxyl groups on the bacterial cell wall are deprotonated, which allows for the uptake of cationic silver at a higher rate. They also reported the possibility of silver ions binding onto the ionized carboxyl groups of remnant amino acids present on the bacterial cell wall tissues. A similar phenomenon was reported by Vijayaraghavan et al. [21] for the adsorption of Ni(II) onto *C. glutamicum*. The presence of various functional groups in microbial cell walls, which enables the cell wall to bind a number of metals ions [23], was well documented. The carboxyl group was suspected to be the main binding site for cationic silver in our study.

3.2. Effects of initial Ag^+ concentration and contact time on biosorption

Fig. 2 shows the effect of the initial Ag^+ concentration on the biosorption capacity of active and inactive *C. glutamicum*. The specific uptake of both active and inactive cells of *C. glutamicum* was

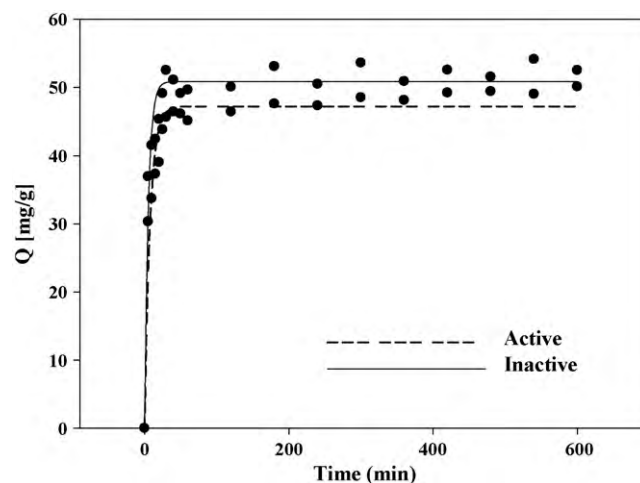


Fig. 2. Effect of contact time on silver adsorption by active and inactive *Corynebacterium glutamicum* biomasses. The lines are outputs of the first-order kinetic model.

found to increase with an increase in contact time and the initial Ag^+ concentration. The time to reach equilibrium was almost the same for both of the studied biosorbents. However, the inactive biomass demonstrated a higher uptake of silver ions comparatively. The maximum uptake by active cells was found to be 50.1 mg/g where as the maximum uptake by inactive cells was found to be 52.5 mg/g for an initial concentration of 1000 mg/L. The high adsorption capacity of the inactive biomass might be due to the fact that while autoclaving, the live cells rupture due to the very high temperature of 121 °C [24,25]. Cell surfaces are mainly anionic due to the presence of ionized groups such as carboxylate, hydroxyl and phosphate groups in the various cell wall polymers. Autoclaving might have led to the exposure to the outer surface of various other functional groups present inside the cell, thereby increasing the access of the Ag^+ to the various binding sites [24,26,27]. These results indicated that more Ag^+ ions could be bound by ruptured cell wall tissues or exposed cell organelles.

When the Ag^+ concentration in the test solution was increased from 100 to 1000 mg/L, the silver uptakes for the active and inactive biomasses were found to increase from 9.71 to 50.1 mg/g and from 9.92 to 52.5 mg/g, respectively. Most of Ag^+ was sequestered from the solution within 30 min after the start of each experiment, beyond which time the concentration of Ag^+ in the liquid phase remained almost constant. Therefore, it is evident that equilibrium was reached within 30 min by live and autoclaved bacterial cells at the studied concentration. The nature of the biosorption process depends on the physical and chemical characteristics of the adsorbent and also on the system conditions. The initial rapid phase might be due to the availability of a higher number of biosorption/vacant sites during the initial stage, as a result of which, there is an increased concentration gradient between the adsorbate in the solution and the adsorbent [28].

3.3. Biosorption dynamics

The sorption kinetics is an important parameter in wastewater treatment as it provides valuable insights into the reaction pathways and mechanisms of the sorption reactions [21]. As noted above, equilibrium was achieved within 30 min, which was very quick when compared to other bacterial sorbents [13,28]. The time it takes to reach equilibrium is one of the important considerations in the design of water and wastewater treatment systems, because it influences the size of the reactor and thereby the economics of the plant [27].

Table 1
Kinetic parameters for the adsorption of silver ions by active and inactive *C. glutamicum* biomasses.

Parameters	Active biomass (mg/g)	Inactive biomass (mg/g)
Experimental Q_e	50.04	52.54
Predicted Q_e	47.19 ± 0.743	50.86 ± 0.706
K_1	0.133	0.195
R^2	0.949	0.954

The experimental biosorption kinetic data was modeled using pseudo first-order kinetics, which can be represented in its non-linear form by the following equation:

$$Q_t = Q_e(1 - \exp(-k_1 t)) \quad (2)$$

where Q_e is the amount of solute sorbed at equilibrium (mg/g), Q_t is the amount of solute sorbed at time t (mg/g), and k_1 is the first-order equilibrium rate constant (min^{-1}). For the Lagergren first-order plot, correlation coefficients were found to be around 0.95 for both of the sorbents studied. Similarly, the calculated Q_e values were close to the experimental Q_e values (Table 1) for both the active and inactive biomasses. This therefore provides validation to the model for the kinetic data of the initial concentrations examined.

3.4. Biosorption equilibrium study

In order to optimize the design of a biosorption system, it is important to establish the most appropriate correlation for the equilibrium curves. Various isotherm equations have been used to describe the equilibrium nature of biosorption. Those equations include the Langmuir and Freundlich equations.

Langmuir equation is represented as follows:

$$Q = \frac{Q_{\max} b_L C_f}{1 + b_L C_f} \quad (3)$$

where Q_{\max} is the maximum silver uptake (mg/g) and b_L is the Langmuir equilibrium constant (L/mg). Langmuir model served to estimate the maximum silver ion uptake values for the sorbents, when those values could not be reached in the experiments (Fig. 3). Both Q_{\max} and b_L were found to be higher for inactive biomass than active biomass (Table 2). High values of b_L were reflected in the steep initial slope of the sorption isotherm, indicating desirable high affinity. Therefore, in general, a high Q_{\max} and a steep initial isotherm slope are desirable for good biosorbents [28,29].

Freundlich equation is represented as follows:

$$Q = K_F C_f^{1/n_F} \quad (4)$$

where K_F is the Freundlich constant (L/g) and n_F is the Freundlich exponent. The Freundlich isotherm study shows, both the K_F and $1/n_F$ values were found to be higher for inactive biomass than active biomass, and therefore it was inferred to mean that the binding capacity was higher for the inactive biomass (Table 2). The Freundlich model also showed a good correlation value comparatively,

Table 2
Isotherm constants of two-parameter models for adsorption of silver ions by active and inactive *Corynebacterium glutamicum* biomasses.

Two-parameter models		Active biomass (mg/g)	Inactive biomass (mg/g)
Langmuir	Q_{\max}	43.2716 ± 4.276	47.1328 ± 4.196
	b_L	0.0212	0.0229
	R^2	0.8552	0.8830
Freundlich	K_F	5.7118	6.2700
	n_F	3.0761	3.0488
	R^2	0.9638	0.9524

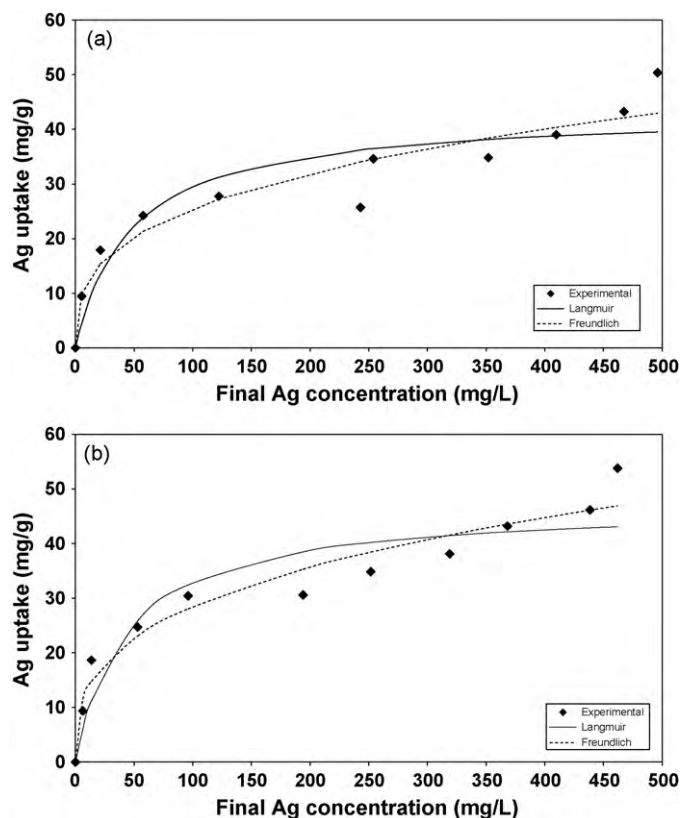


Fig. 3. Two-parameter isotherm models for adsorption of silver ions by (a) active and (b) inactive *Corynebacterium glutamicum* biomasses.

which indicates that the model fits the present experimental data well (Fig. 3).

In case of Ag uptake pattern, a sudden high uptake was noticed at higher initial concentrations of Ag by both active and inactive cells, which we believe could be due to reduction process at high initial Ag concentrations.

3.5. Bioreduction of Ag^+ ions

The silver ions were reduced to nanoparticles after incubation of the silver nitrate with active and inactive biomass for 72 h. To confirm the formation of silver nanoparticles in the suspensions, the suspensions were first analyzed using UV–vis spectroscopy [30–33]. The samples were analyzed every 24 h by the UV–vis spectrometer in order to compare the formation of silver nanoparticles. Peak intensity increased with an increase in time (data not given). The light absorption of silver nanoparticles was monitored in the range of 200–700 nm. No prominent, sharp peak was observed for the silver nanoparticles in the presence of the bacterial cells. A broad peak in the range of 350 and 680 nm was seen instead. This could be attributed to the interference of the bacterial cells in masking the physiochemical and optical properties of the silver nanoparticles in water. Therefore, the plasmon resonance was not clearly observed for silver nanoparticles in the presence of the bacterial cells. After sonication of the cells for 1 h, the cell debris was separated from the solution using a mixed cellulose ester filter (MFS, Japan) with a 0.45 μm pore size and the separated supernatant was analyzed for the presence of nanoparticles using a UV–vis spectrometer. Fig. 4 shows the UV–vis spectrum for the silver nanoparticles produced by active and inactive cells of *C. glutamicum*. Strong plasmon resonance was observed between 400 and 450 nm for our samples obtained from the active and inactive cells, thus indicating the presence of silver nanoparticles in

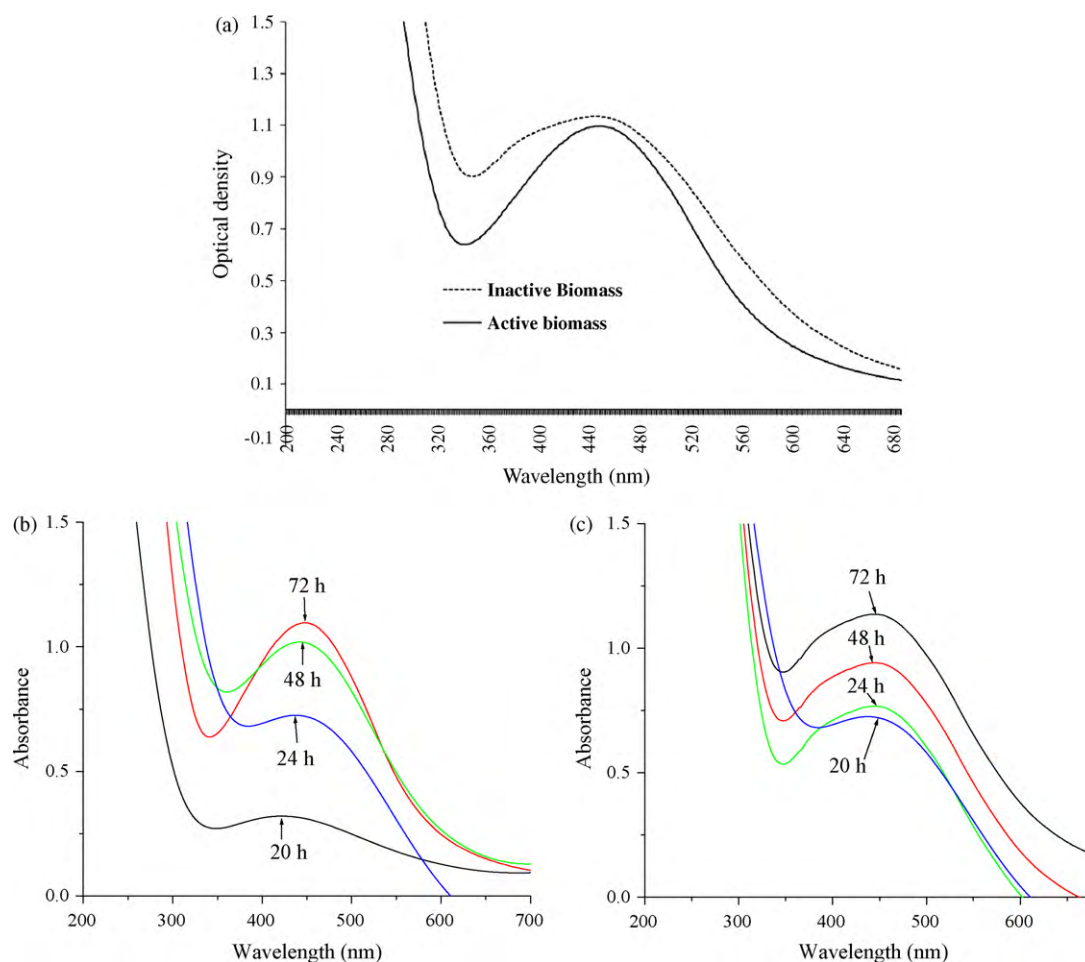


Fig. 4. UV-vis spectra of silver nanoparticles (a) using active and inactive *Corynebacterium glutamicum* biomasses after 72 h of reaction (b) reaction kinetics of silver nanoparticles using active biomass and (c) kinetics of silver nanoparticles using inactive biomasses.

the solution. Even after three weeks, the peak remained close to 440 nm. This indicated that the nanoparticles were well dispersed and that there was not much aggregation [19,20]. After a few days, it was observed that the color of the solution changed from a pale yellow to a brown color which may be due to the excitation of surface plasmon vibrations which is a peculiar property of the silver nanoparticles [34]. The color intensity of inactive biomass was higher than that of active biomass, which is a clear representation of high nanoparticle content in the inactive biomass suspension (Fig. 5). The peak area and height of the UV-vis spectrum obtained for the inactive sorbent was also comparatively higher, which confirms the higher productivity of silver nanoparticles. It was assumed that this higher productivity could be attributed to the higher organic content (as reducing agents) present in the inactive cells due to autoclaving. To confirm the presumption, total organic carbon (TOC) was analyzed for both the active and inactive biomasses. The results indicated that the active biomass contained 1395 mg/L of TOC and the inactive biomass contained 2599 mg/L, which is almost twice the amount of the former. TOC of inactive is higher possibly because the water content of the cell has been got rid of by way of rupturing the cells. So the weight is mostly contributed by cell wall and cell membrane. The chemical groups attached are more accessible to the silver ions and hence the higher amount of reduction, whereas in case of active cells the cell wall is intact and thereby the cell contents too intact leading to less availability of chemical/functional groups capable of reducing silver ions. This result clearly illustrates that autoclaving leads to a release of organics from the cells due to the rupturing of the cell walls.

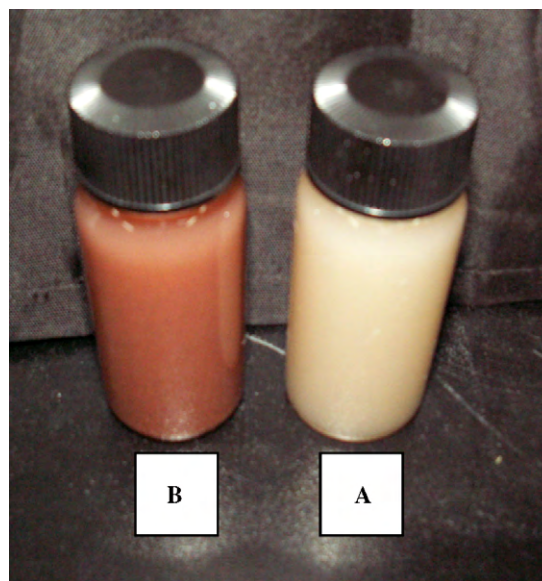
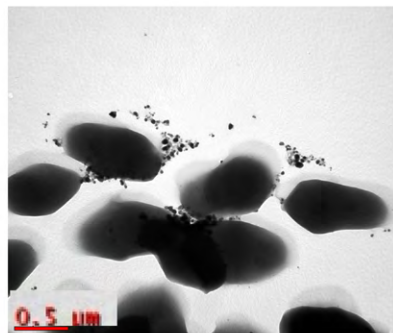
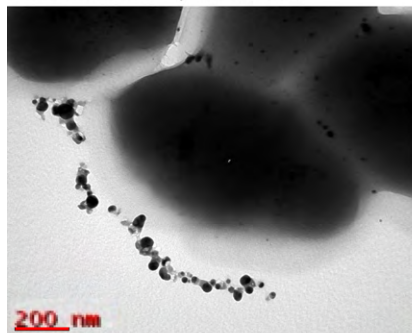


Fig. 5. Photographic images of Ag nanoparticle suspensions after 72 h of reaction (a) active and (b) inactive *Corynebacterium glutamicum* biomasses.

(a) Bioreduction by active cells



(b) Bioreduction by inactive cells

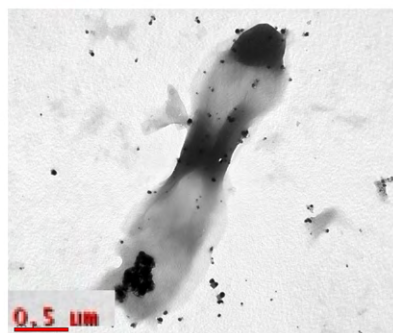


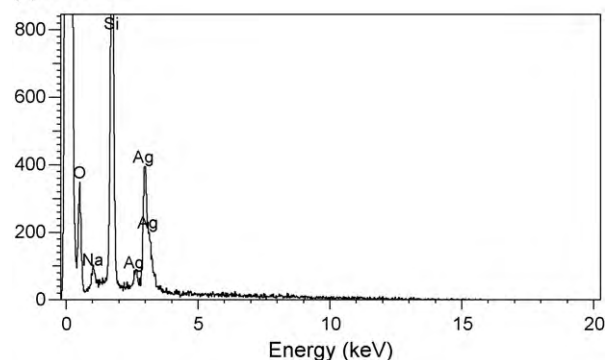
Fig. 6. TEM images of Ag nanoparticles after 72 h of reaction (a) active and (b) inactive *Corynebacterium glutamicum* biomasses.

In addition to the peak at 440 nm, some minor peaks were observed around 380 nm, especially in the case of the inactive biomass. These peaks may be due to the ellipsoidal-shaped particles. Shankar et al. [35] reported that the peak at 370 nm corresponds to the transverse plasmon vibration in the Ag nanoparticles, whereas the peak at 440 nm was due to the excitation of longitudinal plasmon vibrations. Shankar et al. [35] also reported quasi-linear superstructures of the nanoparticles when geranium leaf extract was used as the biomaterial.

3.5.1. Characterization of silver nanoparticles

3.5.1.1. TEM and UV spectrum analysis. The nanoparticles that were produced were observed under the transmission electron microscope (TEM). The TEM images helped us to clearly distinguish the nanoparticle formation by active and inactive cells (Fig. 6). After formation of the nanoparticles, the inactive cell suspension appeared more turbid than the active cell suspension. Notably, the TEM images indicated a clear-cut difference in the nanoparticle formation by active and inactive cells. The active cells had little or no bioreduction on the cell surface. These results indicated that bioreduction in the active cells occurred in the presence of enzymes, organics, inorganic material and other metabolites in the solution that were secreted by active cells in the vicinity of the silver ions during the initial stages. Active cells may require the assistance of various intracellular or extracellular and organic or inorganic substances for the transport of metals across the cell membrane. In contrast, the inactive cells had the formation of nanoparticles on the cell surface and in the solution as well (Fig. 6). This might be because the rupturing of active cells by heat while autoclaving would have exposed various internal organic groups on to the cell surface and release some into the solution as well, thereby facilitating additional binding sites both on the cell surface and in the solution phase. The particles thus formed were very irregular in shape and the size of the nanoparticles ranged from 5 to 50 nm in size. Microbial cell membranes offer a large number of active functional groups and some physiochemical mechanisms of interactions that propa-

(a) Counts



(b) Counts

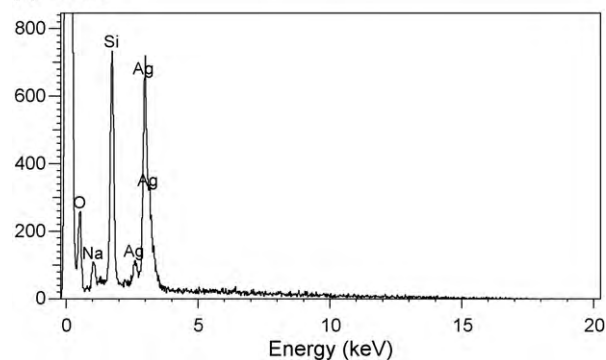


Fig. 7. Energy dispersive X-ray spectrum of silver nanoparticles after 72 h of reaction (a) active and (b) inactive *Corynebacterium glutamicum* biomasses.

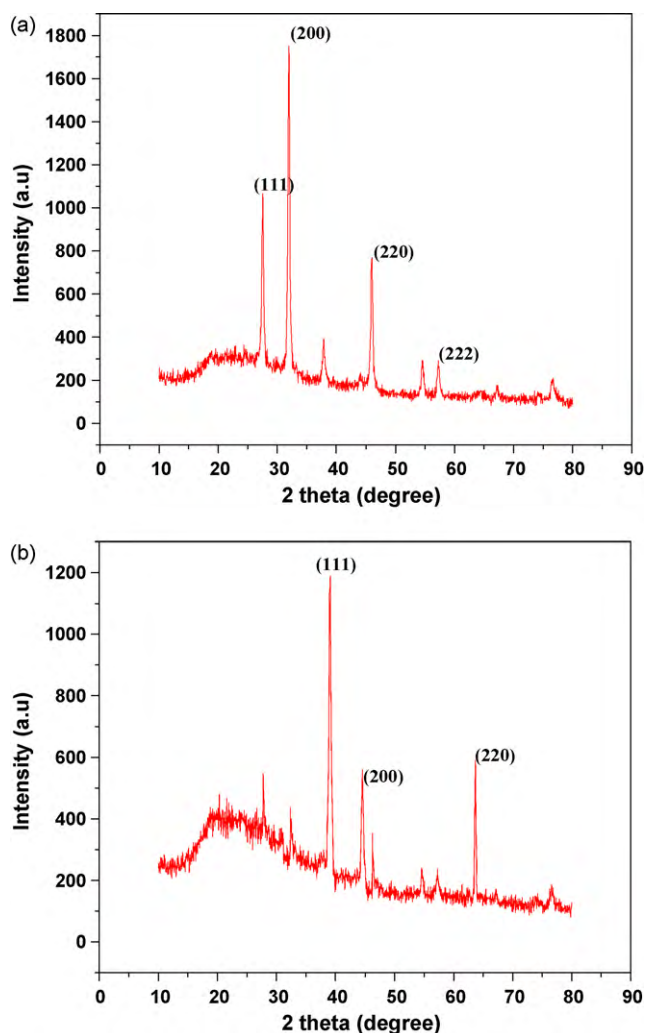


Fig. 8. X-ray diffraction of Ag nanoparticles after 72 h of reaction (a) active and (b) inactive *Corynebacterium glutamicum* biomasses.

gate the transport of metal ions and other substances across the cell membrane. Active cells may also be metal specific and therefore some microbes may secrete metabolites that block the transport of the metal ions across their cell membranes [36]. The membrane transport system of a cell not only controls access to intracellular target sites, but also determines the rate of uptake [37]. Various transport proteins in the cell play a critical role in the development of metal selectivity and resistance to metals [38]. Therefore, the transport of metals in active cells depends on the level of their metabolic activity. Since the concentration of silver was extremely high in our study, it might have caused the rapid death of the cells. Therefore, the metabolic activity of the active cells no longer existed and the reduction of silver ions was completely dependent on the metabolites and organics already present. Meanwhile, in the case of the inactive cells, a large amount of organics was already released during autoclaving. In addition, it is clear from the biosorption studies that the amount of silver ions on the cell surface is higher for inactive cells than active cells and therefore there is more silver available for reduction. The nanoparticles produced and separated by sonication were stored in aqueous medium for a month and then tested for stability which revealed that the nanoparticles were still dispersed and remained intact.

3.5.1.2. EDX and XRD analysis. EDX spectroscopy results confirmed the considerable amount of silver in both active and inactive

biomass (Fig. 7). It also confirmed higher Ag content in the inactive biomass than the active biomass. The optical absorption peak was observed at approximately 3 keV, which is typical for the absorption of metallic silver nanocrystallites due to surface plasmon resonance [39].

Additional studies were carried out using X-ray diffraction (XRD) analysis to confirm the crystalline nature of the nanoparticles (Fig. 8). X-ray powder diffraction patterns were compared to the reference database for metallic silver. The XRD pattern of inactive cells have shown clear peaks of cubic phases (JCPDS No. 03-0921) at 38.7 (111), 44.5 (200) and 64.1 (220). Active cells are not reducing it to pure crystalline silver but to crystalline silver chloride. The XRD analysis of active cells shows clear peaks of silver chloride nanoparticles with cubic phases (JCPDS No. 31-1238) at 27.8 (111), 32 (200), 46 (220) and 54.5 (222). In addition to the peak corresponding of silver, a few other peaks were also obtained in the case of both active and inactive cells. These peaks indicated that some crystalline compounds other than silver were also present in the final system. These products probably originated from the raw material/nutrient source used for bacterial growth. Kumar et al. [40] reported a similar result of additional crystalline impurity peaks for the nitrate reductase mediated synthesis of silver nanocrystals. Therefore, the formation of silver nanocrystals was confirmed by the above-mentioned basic analytical studies.

4. Conclusions

Our study on the biosorption and bioreduction of silver ions by active and inactive cells of *C. glutamicum* has shown that the inactive cells are more efficient in the uptake of silver ions and its subsequent reduction to nanocrystals. The results of our studies indicated the formation of nanoparticles even in the absence of reducing enzymes and it was also demonstrated that organics can propel and assist the bioreduction of metal ions to nanoparticles. Both active and inactive cells are efficient nanofactories. However, the ease of handling dead/inactive *C. glutamicum* and its ample availability as a fermentation waste make it a good choice for the recovery of silver from industrial effluent. The exact mechanism for the bioreduction of nanoparticles is still unknown, but the use of microbes for the efficient recovery, as a nanocrystal, of metals from waste is an interesting prospect in the field of bioremediation. Active and inactive cells containing nanoparticles on their surface can be used as the foundation for various applications in material chemistry. The nanoparticles produced extracellularly can be separated from the cells and can be used as separate particles depending on the application. In this study, we have explored the possible crystallization of silver ions from aqueous solutions by both active and inactive biomass which could form a platform for a cost effective and eco-friendly technique to remove or recover noble metals from industrial and mining wastewaters.

Acknowledgements

This work was supported by NRF grant (NRL ROA-2008-000-20117-0 and WCU R31-2008-000-20029-0) and in part supported by KEITI funded by the Korea government. We thank Mr. J.-G. Kang, Center for University-wide research facilities, for TEM analysis.

References

- [1] A.V. Pethkar, K.M. Paknikar, Thiosulfate biodegradation–silver biosorption process for the treatment of photofilm processing water, *Process Biochem.* 38 (2003) 855–860.
- [2] A. Kapoor, T. Viraraghavan, Fungal biosorption—an alternative treatment option for heavy metal bearing waste waters: a review, *Bioresour. Technol.* 53 (1995) 195–206.

- [3] S.S. Ahluwalia, D. Goyal, Microbial and plant derived biomass removal of heavy metals from waste water, *Bioresour. Technol.* 98 (2006) 2243–2257.
- [4] D. Mohan, C.U. Pittman Jr., Arsenic removal from water/wastewater using adsorbents—a critical review, *J. Hazard. Mater.* 142 (2007) 1–53.
- [5] P.A. Goddard, A.T. Bull, The isolation and characterisation of bacteria capable of accumulating silver, *Appl. Microbiol. Biotechnol.* 31 (1989) 308–313.
- [6] A.V. Pethkar, S.K. Kulkarni, K.M. Paknikar, Comparative studies on metal biosorption by two strains of *Cladosporium cladosporioides*, *Bioresour. Technol.* 80 (2001) 211–215.
- [7] N.C.M. Gomes, C.A. Rosa, P.F. Pimentel, L.C.S. Mendonça-Hagler, Uptake of free and complexed silver ions by different strains of *Rhodotorula mucilaginosa*, *Braz. J. Microbiol.* 33 (2002) 62–66.
- [8] D. Mandal, M.E. Bolander, D. Mukhopadhyay, G. Sarkar, P. Mukherjee, The use of microbes for formation of metal nanoparticles and their application, *Appl. Microbiol. Biotechnol.* 69 (2006) 485–492.
- [9] M. Sathishkumar, K. Sneha, Y.-S. Yun, Immobilization of silver nanoparticles synthesized using *Curcuma longa* tuber powder and extract on cotton cloth for bactericidal activity, *Bioresour. Technol.* doi:10.1016/j.biortech.2010.05.051.
- [10] B. Narayanan, N. Saktivel, Biological synthesis of metal nanoparticles, *Adv. Colloid Interface Sci.* 156 (2010) 1–13.
- [11] K. Simkiss, K.M. Wilbur, *Biomimetalization*, Academic press, New York, 1989.
- [12] S. Mann, *Biomimetic Materials Chemistry*, VCH, New York, 1996.
- [13] H. Zhang, Q. Li, Y. Lu, D. Sun, X. Lin, X. Deng, N. He, S. Zheng, Biosorption and bioreduction of diamine silver complex by *Corynebacterium*, *J. Chem. Technol. Biotechnol.* 80 (2005) 285–290.
- [14] Z.Y. Lin, J.K. Fu, J.M. Wu, Y.Y. Liu, H. Cheng, Preliminary study on the mechanism of non-enzymatic bioreduction of precious metal ions, *Acta Phys. Chim. Sin.* 17 (2001) 477–480.
- [15] F. Mouxing, L. Qingbiao, S. Daohua, L. Yinghua, H. Ning, D. Xu, W. Huixuan, H. Jiale, Rapid preparation process of silver nanoparticles by bioreduction and their characterizations, *Chinese J. Chem. Eng.* 14 (2006) 114–117.
- [16] J.K. Fu, W.D. Zhang, Y.Y. Liu, Z.Y. Lin, B.X. Yao, S.Z. Weng, J.L. Zeng, Characterization of adsorption and reduction of noble metal ions by bacteria, *Chem. J. Chinese Univ.* 20 (1999) 1452–1454.
- [17] J.K. Fu, Y.Y. Liu, P. Gu, D.L. Tang, Z.Y. Lin, B.X. Yao, S.Z. Weng, Spectroscopic characterization on the biosorption and reduction of Ag(I) by *Lactobacillus* sp. A09, *Acta Phys. Chem. Sin.* 16 (2000) 770–782.
- [18] A. Ahmad, P. Mukherjee, S. Senapati, D. Mandal, M.I. Khan, R. Kumar, M. Sastry, Extracellular biosynthesis of silver nanoparticles using the fungus *Fusarium oxysporum*, *Colloids Surf. B* 28 (2003) 313–318.
- [19] A.R. Binupriya, M. Sathishkumar, S.-I. Yun, Myco-crystallization of silver ions to nanosized particles by live and dead cell filtrates of *Aspergillus oryzae* var. *viridis* and its bactericidal activity toward *Staphylococcus aureus* KCCM 12256, *Ind. Eng. Chem. Res.* 49 (2010) 852–858.
- [20] A.R. Binupriya, M. Sathishkumar, K. Vijayaraghavan, S.-I. Yun, Bioreduction of trivalent aurum to nano-crystalline gold particles by active and inactive cells and cell-free extract of *Aspergillus oryzae* var. *viridis*, *J. Hazard. Mater.* 177 (2010) 539–545.
- [21] K. Vijayaraghavan, M.W. Lee, Y.S. Yun, Evaluation of fermentation waste (*Corynebacterium glutamicum*) as a biosorbent for the treatment of nickel(II)-bearing solutions, *Biochem. Eng. J.* 41 (2008) 228–233.
- [22] Z. Lin, C. Zhou, J. Wu, J. Zhou, W. Lin, Further insight into the mechanism of Ag⁺ biosorption by *Lactobacillus* sp. strain A09, *Spectrochim. Acta Part A* 61 (2005) 1195–1200.
- [23] T. Robinson, G. McMullan, R. Marchant, P. Nigam, Remediation of dyes in textile effluent: a critical review on current treatment technologies with a proposed alternative, *Bioresour. Technol.* 77 (2001) 247–255.
- [24] M. Sathishkumar, G.S. Murugesan, P.M. Ayyasamy, K. Swaminathan, P. Lakshmanaperumalasamy, Bioremediation of arsenic contaminated groundwater by modified mycelia pellets of *Aspergillus fumigatus*, *Bull. Environ. Contamin. Toxicol.* 72 (2004) 617–624.
- [25] M. Sathishkumar, A.R. Binupriya, K. Swaminathan, J.G. Choi, S.E. Yun, Arsenite sorption in liquid-phase by *Aspergillus fumigatus*: adsorption rates and isotherm studies, *World J. Microbiol. Biotechnol.* 24 (2008) 1813–1822.
- [26] M.N. Hughes, R.K. Poole, *Metals and Microorganisms*, Chapman and Hall Publishers, London, 1989.
- [27] K.K. Deepa, M. Sathishkumar, A.R. Binupriya, G.S. Murugesan, K. Swaminathan, S.E. Yun, Sorption of Cr(VI) from dilute solutions and wastewater by live and pretreated biomass of *Aspergillus flavus*, *Chemosphere* 62 (2006) 833–840.
- [28] M. Sathishkumar, A.R. Binupriya, D. Kavitha, S.E. Yun, Kinetic and isothermal studies on 2,4-dichlorophenol by palm pith carbon, *Bioresour. Technol.* 98 (2007) 866–873.
- [29] I. Langmuir, The adsorption of gases on plane surfaces of glass, mica and platinum, *J. Am. Chem. Soc.* 40 (1918) 1361.
- [30] A. Henglein, Physicochemical properties of small metal particles in solution: “microelectrode” reactions, chemisorption, composite metal particles, and the atom-to-metal transition, *J. Phys. Chem.* 97 (1993) 5457–5471.
- [31] M. Sastry, K.S. Mayya, K. Bandyopadhyay, pH dependent changes in the optical properties of carboxylic acid derivatized silver colloidal particles, *Colloids Surf. A* 127 (1997) 221–228.
- [32] M. Sastry, V. Patil, S.R. Sainkar, Electrostatically controlled diffusion of carboxylic acid derivatized silver colloidal particles in thermally evaporated fatty amine films, *J. Phys. Chem. B* 102 (1998) 1404–1410.
- [33] M. Sastry, A. Ahmad, M.I. Khan, R. Kumar, Biosynthesis of metal nanoparticles using fungi and actinomycete, *Curr. Sci.* 85 (2003) 162–170.
- [34] K.C. Bhaisa, S.F. D'Souza, Extracellular biosynthesis of silver nanoparticles using the fungus *Aspergillus fumigatus*, *Colloids Surf. B* 47 (2006) 160–164.
- [35] S.S. Shankar, A. Ahmad, M. Sastry, Geranium leaf assisted biosynthesis of silver nanoparticles, *Biotechnol. Prog.* 19 (2003) 1627–1631.
- [36] M.E. Blaza, Z.A. Shaikh, Calcium and mercury accumulation in rat hepatocytes, *Toxicol. Appl. Pharmacol.* 113 (1992) 118–125.
- [37] E.C. Foulkes, Transport of toxic heavy metals across cell membranes, *Exp. Biol. Med.* 22 (2000) 234–240.
- [38] I.T. Paulsen, M.H. Saier Jr., A novel family of ubiquitous heavy metal ion transport protein, *J. Membr. Biol.* 156 (1997) 99–103.
- [39] K. Kalimuthu, R.S. Babu, D. Venkataraman, M. Bilal, S. Gurunathan, Biosynthesis of silver nanocrystals by *Bacillus licheniformis*, *Colloids Surf. B: Biointerfaces* 65 (2008) 150–153.
- [40] S.A. Kumar, M.K. Abyaneh, S.W. Gosavi, S.K. Kulkarni, R. Pasricha, A. Ahmad, M.I. Khan, Nitrate reductase-mediated synthesis of silver nanoparticles from AgNO₃, *Biotechnol. Lett.* 29 (2007) 439–445.